## **Current Research and Innovations Journal**

#### **Research Article**

# OFFSHORE WIND TURBINES AND THEIR ROCKING DYNAMICS: A SIMULATION-BASED INVESTIGATION

#### Xiaolong Wei Zhang

Sinopec Engineering Incorporation, Chaoyang District, Beijing, 100101, China DOI: 10.5281/zenodo.14678016

#### **Abstract**

The design of efficient wind turbines is crucial for harnessing wind energy effectively. Central to this design process is the consideration of wind speed distribution, which significantly impacts the frequency of load conditions under various design scenarios. In this study, we explore the fundamental relationship between wind power and wind speed, emphasizing the role of key factors such as air density, turbine area, and wind speed. While Betz's law provides an essential framework for estimating the maximum power that can be extracted from the wind, it is important to acknowledge its limitations. The Betz's model, which suggests that an ideal turbine can capture 16/27 of the available wind power, is a simplification that does not account for various practical factors, including wake rotation, variable geometry effects, and aerodynamic considerations.

Keywords: Wind Turbine Design, Wind Speed Distribution, Wind Power Equation, Betz's Law, Aerodynamic Effects

#### 1. Introduction

#### 1.1 The energy and power in the wind

In the process of designing wind turbine, the wind speed distribution is a very remarkable factor to pay attention to. The speed distribution will affect the frequency of occurrence of each load condition in different normal design situation.

The equation of wind power is,

$$P_{wind} = \frac{\rho}{2} A_{turb} v_t^3, \tag{1}$$

where  $\rho$  is the density of the air,  $A_{turb}$  is the area which the air passes through,  $v_t$  is wind speed.

According to the Betz's law, an ideal turbine can extract 16/27 of the above wind power. Actually, the Betz's model is not a perfect model, because the many other factors should be taken into account, such as wake rotation, the effect of variable geometry and aerodynamic effect.

In practice, Neammanee et al (2007) [2] states that the non-laminar air flow and friction occur on the surface of the wind blade. The real output extracted by a wind turbine can be calculated by equation,

$$P_{wind} = 0.5C_p \rho A_{turb} v_t^3, \tag{2}$$

Where  $CC_{pp}$  is illustrated as a power coefficient, also known as the Bezt factor, is obtained by,

$$C_p = \frac{rotor\ power}{power\ of\ wind},\tag{3}$$

where  $\rho$  is the air density,  $A_{turb}$  is the rotor swept area,  $v_t$  is the wind speed

| ISSN: 3065-0712 Page | 36

## **Current Research and Innovations Journal**

#### **Research Article**

It does not mean the longer the blade is, the more power the turbine will produce. The induced gravity loading will beome challenge to the capacity of the turbines with increasing of the blades.

The pitch angle  $\beta$  can change the amount of the output power by influencing the lift and drag forces generating on the blades. Therefore, another power output equation can be calculated by,

-67-

9

$$P_{turb} = \frac{\rho}{2} \pi R^2 v_t^3 C_p(\lambda, \beta), (4)$$

#### 1.2 Aerodynamic of wind turbine & Theory

As the previous aerodynamic study described, the behavior of the aerodynamic is so unsteady and unpredictable.

1) Airfoil

The following Figure 1 shows Lift & drag vectors and the angle of Attack.

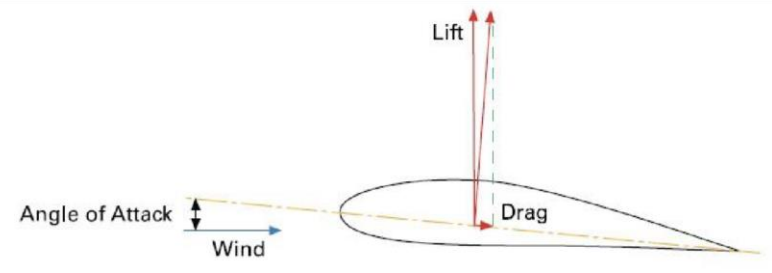
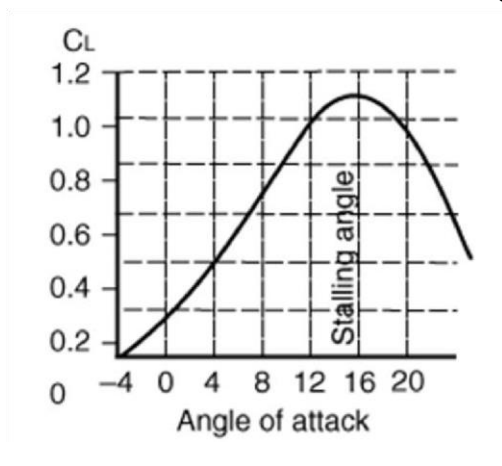


Figure 1: Lift & drag vectors, from WE handbook (no date)[3]

The net result of different forces generated low air pressure and high air pressure is the lift force. With the increase of angle of attack, the lift force is getting bigger in a certain range.

In the wind workshop book of Piggott (1997)<sup>[4]</sup>, one of famous aviation airfoils is NACA series, such as the wing section of NACA4412, in the following Figure 2:



| ISSN: 3065-0712 | Page | 37

## **Current Research and Innovations Journal**

#### **Research Article**

Figure 2 Oncoming air movements (Piggott, 1997)<sup>[4]</sup> The aerospace engineering quantity:

$$CC_{LL} = 2LL/\rho\rho VV^2 SS, \tag{5}$$

where  $C_L$  is lifting coefficient, L is the lift of a whole airplane wing,  $\rho$  is the mass density of the air, V is the free-stream velocity, and S is the wing area; this is also applicable to other airfoils. Hence, aerodynamic lift that varies with the angle of attack ( $\alpha$ ) and the shape of the airfoil.

There is another Figure 3 to simply explain the definitions of the angle of attack  $\alpha$ , the chord length and the direction of relative air movement, as seen by the wind section.

In the Figure 3, with the angle of attack growing, the lift coefficient increases until reaches a point, called "stall". In other word, the lift force increases before reaching "stall" point. After the stall stage, airflow begins to separate off, and generates a turbulence zone, and the lift decreases again. Hence, there exists an optimum angle of attack to obtain the maximum lift. 9

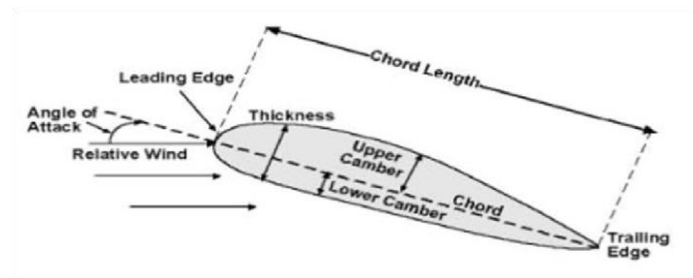


Figure 3 Lift versus angle of attack for the NACA4412 ( $R_{pp} = 10^7$ ) (Piggott, 1997)<sup>[4]</sup>

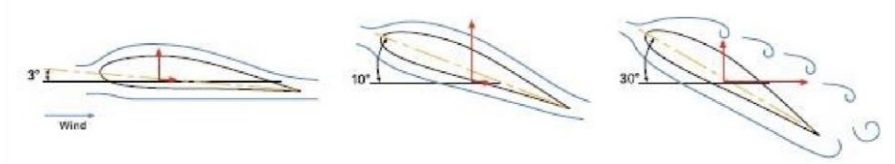


Figure 4 Blade at low, medium & high angles of attack (WE HANDBOOK)<sup>[3]</sup>

The Figure 4 indicates visually the change of the amount of lift, in order to obtain the maximum lift; the optimum angle of attack of the specific airfoil is between  $10^{\circ}$  and  $30^{\circ}$ .

#### 1.3 Computational fluid dynamics (CFD)

Computational fluid dynamics is shorted as CFD, which based on computing numerical methods and algorithms, it is widely used to solve and analyze the fluid problems nowadays. Using CFD methods is time and cost-efficient way to simulate fluid motion. Before operating the real and costly experiments, the CFD software can be applied to simulate.

Generally, the CFD methods contain some basic procedure:

- 1) defining the geometry of the problem,
- 2) meshing the fluid into discrete cells,

| ISSN: 3065-0712

## **Current Research and Innovations Journal**

#### **Research Article**

- defining the physical modeling including the equations, enthalpy, radiation, species conservation and so on,
- 4) defining boundary conditions,
- 5) beginning the simulation, analyzing and visualizing the result by a postprocessor.

#### 2. Methodology

It is necessary to model an improved three-dimensional wind turbine by using finite element method to get better working efficiency. In this chapter, more details and processes of the wind turbine modelling and the structural analysis will be elaborated by using CFD software called Comsol Multiphysics, which is famous for its powerful simulating function. In the wind turbine structure analysis, Comsol Multiphysics will be used to simulate fluid field around rotors, in addition, represent strain and stress distributions on the blades combined with the application of Navier-Stokes equations. Furthermore, Comsol Multiphysics will take the advantage of finite element analysis, which is a numerical solution technique, to deal with numerous physical problems.

The finite element method (FEM) is a numerical method to obtain approximate solutions of different equations, especially for partial differential equation (PDE).

#### 2.1 Initial failure

Initially, the plan was to simulate a realistic wind turbine model, whose tower is 60 m high and blade is more than 30m long. And the air cube was built originally with 150 m length, and the wind turbine was right middle at the bottom of the air cube.

Unfortunately, because of the massive of the mesh elements, only Solid-Stress-Strain module in the 9 model of wind turbine was running well; the model could not simulate the wind field around the rotor.

#### 2.2 Wind turbine modelling

Considering of too many mesh elements to solve, another micro air cube was created by 200  $\mu$ m long, 150  $\mu$ m high and 150  $\mu$ m wide, the miniature wind turbine has a lightly off-center position in the channel. The fluid is air with a density  $\rho$ =1.205kg/m³, and dynamic viscosity  $\eta$ =1.8e<sup>-5</sup> Pa·s. The wind turbine is made of Steel AISI 4340 with a density  $\rho$ =7850 kg/m³ and a Young's modulus E=2.05x10<sup>11</sup>Pa.

The wind turbine model contains a fluid part, which is solved with the Navier-Stokes equations in the fluid cube, and a structural mechanics part. A moving mesh is applied to ensure the flow domain is deformed along with the wind turbine. The application modes and Fluid-Structure-Interaction specific settings on subdomains and boundaries are available directly when using the predefined multiphysics couplings for fluid-structure interaction.

#### 2.3 Arbitrary Lagrangian-Eulerian (ALE)

The theory illustrates how air flow can deform structures and how to solve for the flow in a continuously deforming geometry using the arbitrary Lagrangian-Eulerian (ALE) technique.

| ISSN: 3065-0712 Page | 39

## **Current Research and Innovations Journal**

#### **Research Article**

The model geometry consists of a micro air cube, and wind turbine in the middle, which can be regarded as an obstacle. The fluid flows from left to right, and it imposes a force on the structure's walls, hence the viscous drag and fluid pressure are produced. The structure bends under the applied load. Consequently, the fluid flow passes a new path, thus it would generate incorrect results if the flow is solved in the initial geometry. The ALE technology manages the deforming geometry and moving boundaries by using a moving grid.

#### 2.4 Fluid flow

The fluid flow in the air block is described by the Navier-Stokes equations, solving for the velocity field  $u = (\mu, v)$  and the pressure, p:

$$\rho \frac{\partial \mathbf{u}}{\partial t} - \nabla \cdot [-p \mathbf{I} + \eta (\nabla \mathbf{u} + (\nabla \mathbf{u})^T)] + \rho (\mathbf{u} \cdot \nabla) \mathbf{u} = \mathbf{F}$$

$$-\nabla \cdot \mathbf{u} = 0$$
, (6)

where I is the unit diagonal matrix, F is the volume force affecting the fluid,  $\rho$  is the density and  $\eta$  is the dynamic viscosity. Density, dynamic viscosity and volume force are specified in this research. F, the volume force vector, describes a distributed force field;  $\eta$  is dynamic viscosity, describes relationship between the shear stresses in a fluid and the shear rate;  $\rho$  is the fluid density, depend on material property. The model neglects gravitation and other volume forces affecting the fluid, so F=0.

In terms of fluid boundary conditions, at the inlet, the model uses a fully developed flow, the velocity of wind is assumed as constant, which does not change varying with time. It is specified as the following equation:

$$u = 16 \times U_{max} \times y \times (width - y) * z * (height - z) / (width^2 \times height^2),$$
 (7)

where the U<sub>max</sub> is the maximum inlet velocity, width and height are the channel width and height.

The Navier-Stokes equations are solved in the deformed coordinate system. At the inlet, the model uses a fully developed laminar flow. The frictional stress at all other boundaries is assumed small and negligible, which describes as no-slip conditions, that is u = 0, apply. At the outlet, zero pressure is applied.

In the Boundary Settings dialog box, the following boundary conditions are applied on the active boundaries, like the following Table 1 Boundary Conditions in Incompressible Navier-Stokes Module

Boundary Setting	1.	2	3
Boundary Type	Outlet	Wall	Inlet
Boundary Condition	Pressure, no viscous stress	No slip	Velocity
Uo			16*u_max*y*(width- y)*z*(height-z)/ (width^2*height^2)
Vo			0
Po	0		

| ISSN: 3065-0712

## **Current Research and Innovations Journal**

#### **Research Article**

#### 3. Programme and Methodology

#### 3.1 Structure Mechanics

Due to the viscous and pressure forces exerted by the air, the wind turbine will undergo a deformation. The elastic formulation and nonlinear geometry formulation will be used to deal with the structural deformations. For boundary conditions, the wind turbine is fixed to the bottom of the fluid block, and the tower, the generator and blades are fixed with each other, so they cannot move in any direction.

On the boundaries that are not fixed, apply Fluid load to define the fluid load on the solid domain. The fluid load on all other boundaries is given by:

$$\mathbf{F}_{\mathrm{T}} = -\mathbf{n} \cdot (-p\mathbf{I} + \eta(\nabla \mathbf{u} + (\nabla \mathbf{u})^{T}))$$
(8)

where n is the normal vector to the boundary. This load represents a sum of pressure and viscous forces.

#### 3.2 Wind speed test

A German physicist called Albert Betz concluded in 1919 that no wind turbine can convert more than 16/27 (59.3%) of the kinetic energy of the wind into mechanical energy turning a rotor. The equation of wind power is,

$$P_{wind} = \frac{\rho}{2} A_{turb} v_t^3, \tag{9}$$

where  $\rho$  is the density of the air,  $A_{turb}$  is the area which the air passes through,  $v_t$  is wind speed.

The wind speed in the equation impacts the wind power to a large degree, the higher the wind speed is, the more energy can be obtained. While, the huge wind speed may cause the damages of wind turbines because of the high pressures. Having knowledge of how a turbine behaves in different wind speeds is critical to understand the income lost by any improper design of wind turbines.

In the wind speed test, the following Table 2 has investigated four wind turbine cases to reveal the relationship between the wind speed and the structural response of turbines.

Table 2 All parameters in Case 1, Case 2, Case 3 and Case 4with different maximum wind inlet velocity

Cases	Blades Number	Blades lengths(um)	Max.wind inlet velocity(m/s)
1	3	30	1.5
2	3	30	5
3	3	30	10
4	3	30	15

| ISSN: 3065-0712

# Current Research and Innovations Journal

#### **Research Article**

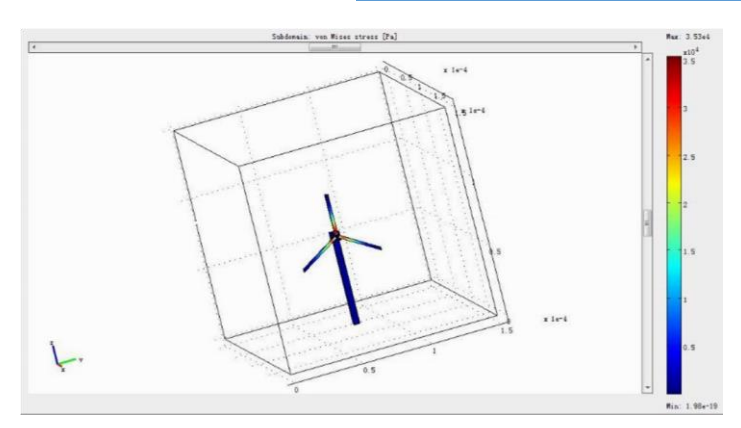


Figure 5 Von Mises Stress in 1.5m/s maximum inlet speed in Case 1

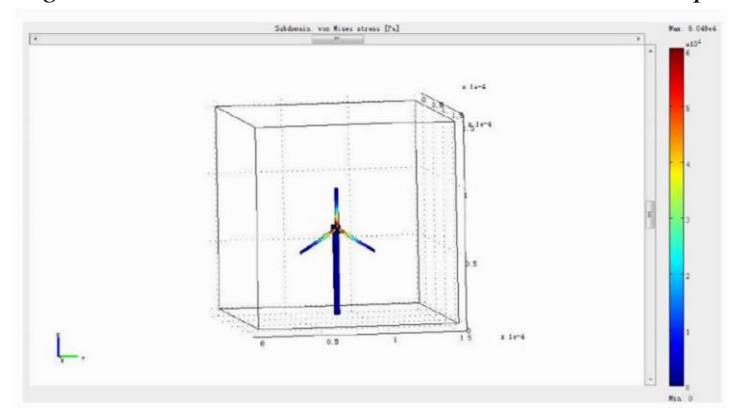


Figure 6 Von Mises Stress in 5m/s maximum inlet speed in Case 2

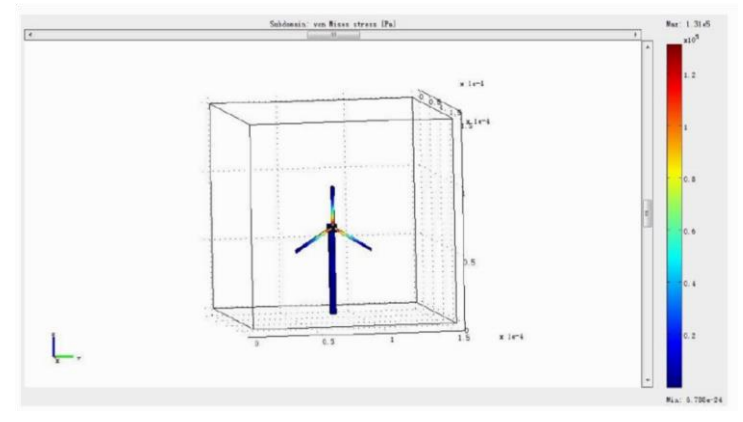


Figure 7 Von Mises Stress in 10m/s maximum inlet speed in Case 3

| ISSN: 3065-0712

### <u>Current Research and Innovations</u> **Journal**

#### **Research Article**

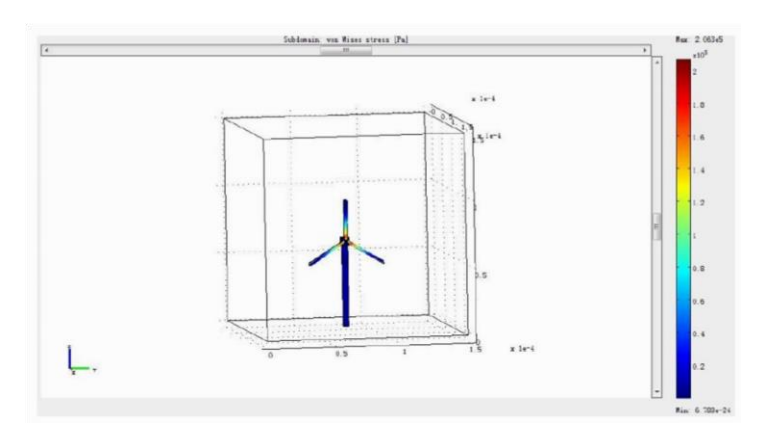


Figure 8 Von Mises Stress in 15m/s maximum inlet speed in Case 4 The Figure 9 below shows Von Mises Stress on turbines with the increase of maximum inlet speed.

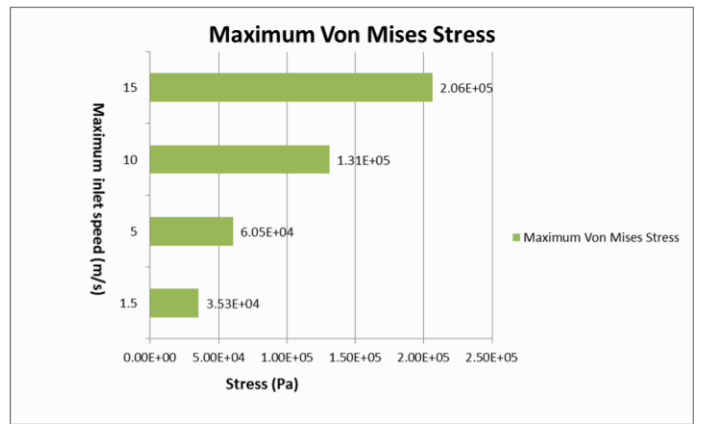


Figure 9 Von Mises Stress on turbines in Case 1, Case 2, Case 3 and Case 4

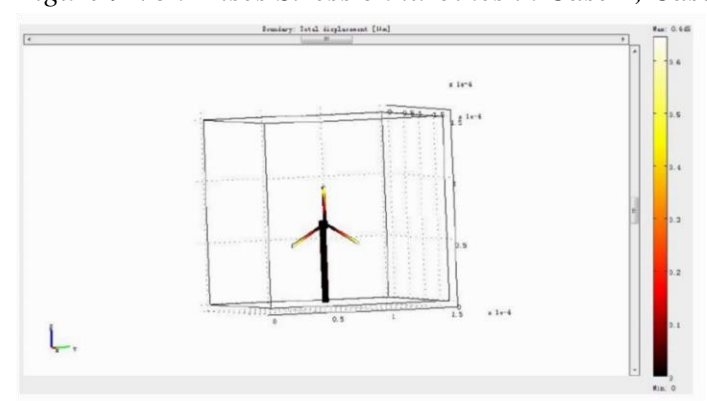


Figure 10 Total displacement in 1.5m/s maximum inlet speed in Case 1

| ISSN: 3065-0712 Page | 43

### <u>Current Research and Innovations</u> <u>Journal</u>

#### **Research Article**

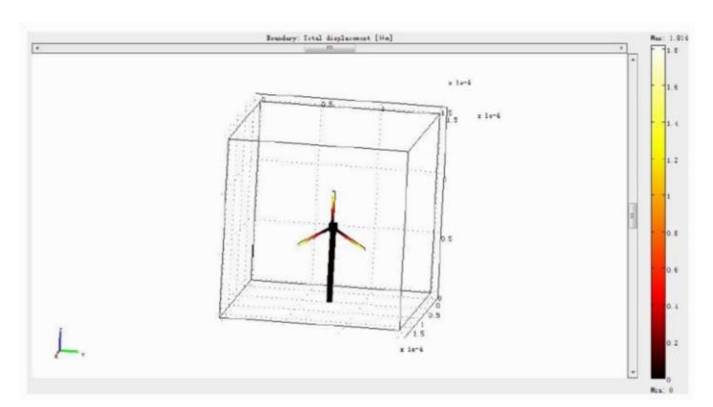


Figure 11 Total displacement in 5m/s maximum inlet speed in Case 2

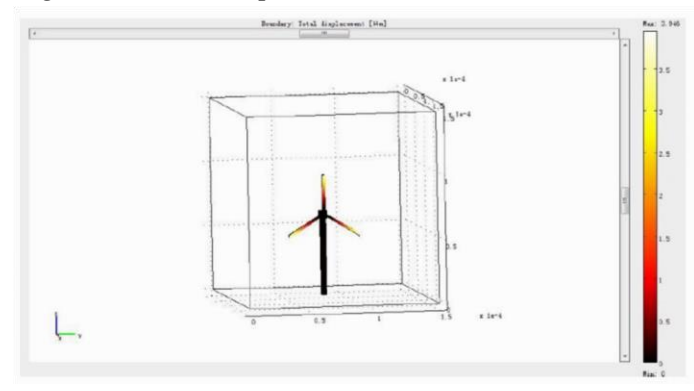


Figure 12 Total displacement in 10m/s maximum inlet speed in Case 3

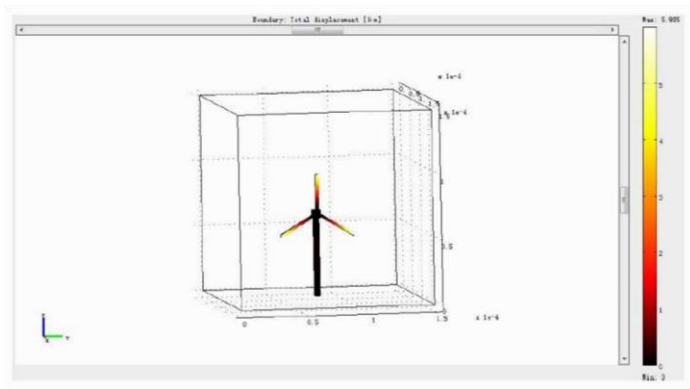


Figure 13 Total displacement in 15m/s maximum inlet speed in Case 4

| ISSN: 3065-0712

### <u>Current Research and Innovations</u> **Journal**

#### **Research Article**

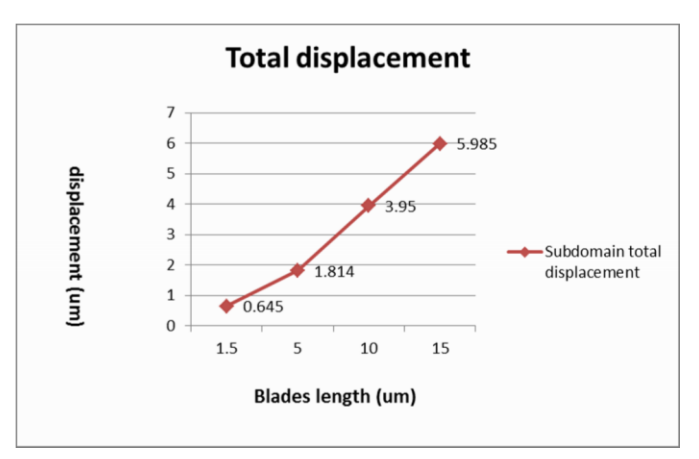


Figure 14 Total displacements on turbines in Case 1, Case 2, Case 3 and Case 4

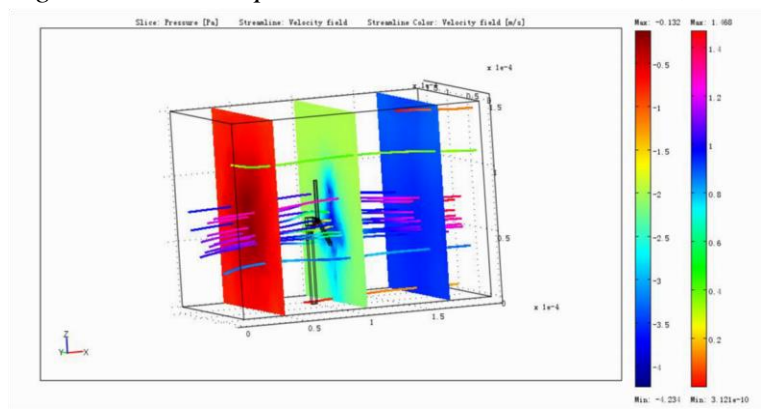


Figure 15 Pressure and streamline in 1.5 m/s maximum inlet speed in Case 1

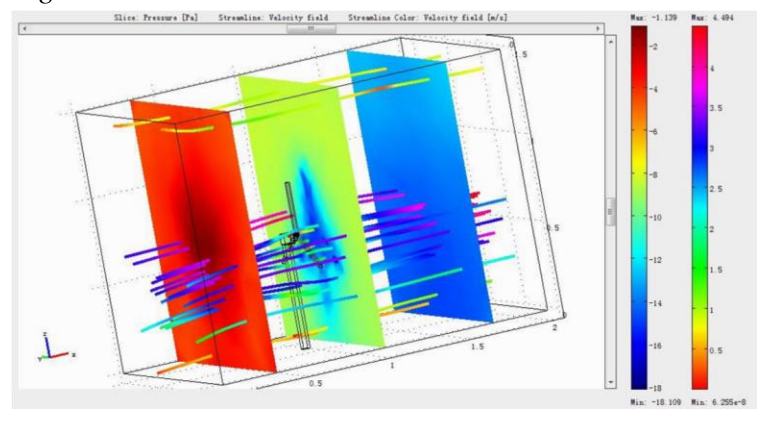


Figure 16 Pressure and streamline in 5 m/s maximum inlet speed in Case 2

| ISSN: 3065-0712 Page | 45

### <u>Current Research and Innovations</u> **Journal**

#### **Research Article**

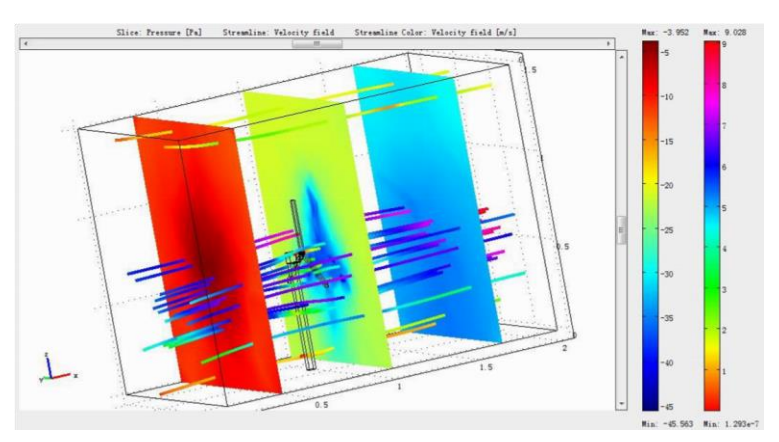


Figure 17 Pressure and streamline in 10 m/s maximum inlet speed in Case 3

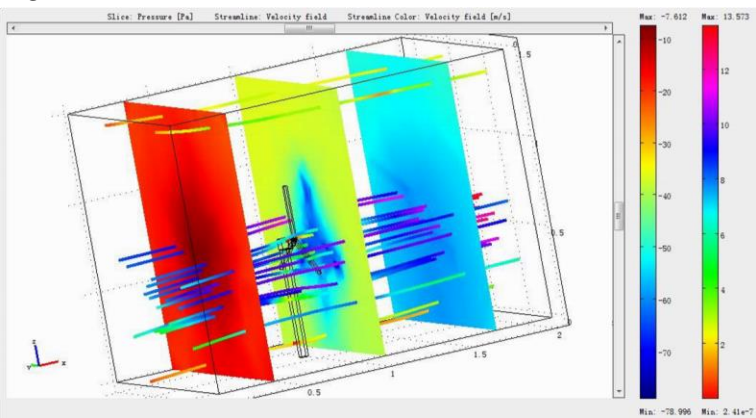


Figure 18 Pressure and streamline in 15 m/s maximum inlet speed in Case 4

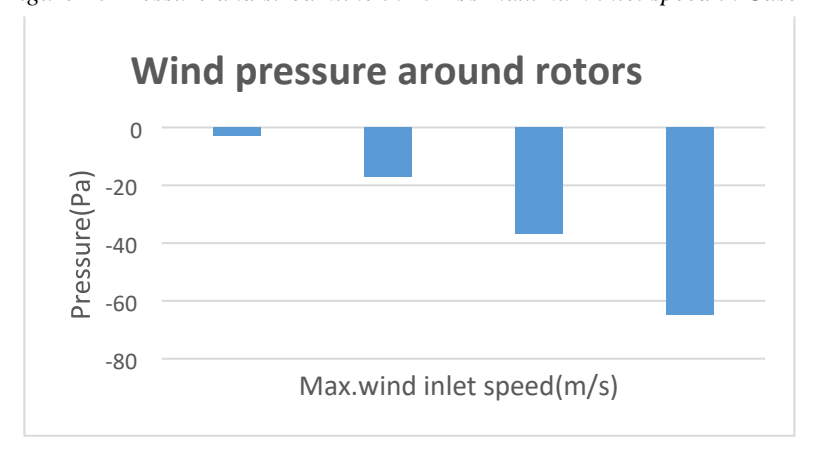


Figure 19 Pressures on turbines in Case 1, Case 2, Case 3 and Case 4
Table 3 All results on blades with different maximum wind inlet velocity in Case 1, Case 2, Case 3 and Case 4

| ISSN: 3065-0712 Page | 46

### <u>Current Research and Innovations</u> <u>Journal</u>

#### **Research Article**

Cases	Max. von mises stress(Pa)	Boundary Total displacement(um)	Wind pressures around rotors(Pa)	Blades lengths(um)	Max.wind inlet velocity(m/s)
1	3.53E+04	0.645	-3.5	30	1.5
2	6.05E+04	1.814	-17	30	5
3	1.31E+05	3.946	-37.5	30	10
4	2.06E+05	5.985	-65	30	15

All the figures show the structural response on turbines and wind pressure changes around rotors. In terms of structural analysis, in Figure 5,6,7,8,10,11,12 and13, all the figures have two gradually increasing trends which are the maximum Von Mises Stress and total displacement when inlet speed grows up. From Figure 14, it can be seen that as the length of the blade increases, the total displacement also increases. Figure 19 reflects that as the maximum wind inlet speed increases, the pressure on the rotors also increase, which is consistent with theory. When maximum inlet speed arrives 15 m/s, the 9

biggest total displacement and maximum Von Mises Stress are obtained on the turbine, which are 5.985 μm and 2.06x 10<sup>5</sup> Pa respectively. When the blade is 30 meters long, Table 3 summarizes other experimental data with different wind speeds to make it clearer. In other word, the effect of wind speed on internal stress and displacement is significant. According to the wind power equation, wind speed has a positive impact on extracted power, the higher the wind speed is, the more energy can be produced. The pressure data around rotors in Figure 15,16,17 and 18 indicate that as the wind speed rise, the wind pressure increase, which may cause wind turbine damages. In summary, the area with high speed wind is preferred to obtain energy in the wind turbine design. However as the wind speed grows up, the high internal stress, the large displacement and the high pressure will make wind turbine damaged, the designer should draw attention to find a balanced and optimized way.

#### 4. Discussion and Conclusions

#### 4.1 Conclusions

Wind speed is a significant factor in the turbine design. Maximum Von Mises Stress and total displacement both increase when wind speed rises. In the mean time, the wind pressure around rotors increases lineally after the wind speed increased, which may cause wind turbine damages. The wind power equation shows that wind has a positive impact on extracted power. Overall, the high wind speed is preferable to produce electricity; on the other hand, it tends to result in high internal stress and high pressure. In terms of choosing location of wind turbines, the designer should pay attention to the advantages and disadvantages to find the optimal solution.

| ISSN: 3065-0712 | Page | 47

### <u>Current Research and Innovations</u> **Journal**

#### **Research Article**

The location choosing of wind turbine is limited by both wind speed and internal stress, so the designer should take both factors into consideration.

#### 4.2 Recommendations of Future Work

In the thesis, the micro wind turbines have been established. However, only the Solid-Stress-Strain module was running well in the real sized wind turbine model(The real sized model has a 150m length air cube, a 60m height tower, and three 30 m length blades), but it failed to simulate the wind field around rotors. The reasons include:

- 1) too many mesh elements cause no convergence,
- 2) too complex wind turbine design results in complicated boundaries to deal with.

In addition, it failed to govern a time-dependent equation to rotate blades as time goes on in the thesis. More researches need to be carried out to obtain a time-dependent governing equation, and the manual adjustment in Solver Parameters.

For the future work, it still has a lot of work to do:

- 1) it's better to simplify the geometry of realistic model,
- 2) to make sure the model runs successfully, it must define the boundary conditions,
- 3) the person who will complete the future work must find out an appropriate time-dependent equation. It is the basic principles of keeping blades rotating.

#### References

- International Electrotechnical Commission (2005) IEC 61400-1 Wind Turbine Part 1: Design Requirements, Third Edition
- Neammanee, B., Sirisumrannukul, S. and Chatratana, S. (2007) Development of a Wind Turbine Simulator for Wind Generator Testing International Energy Journal 8, 21-28.
- WE Handbook-2-Aerodynamics and Loads 8 (no date) Wind turbine[online] Available at. http://www.gurit.com/files/documents/2\_aerodynamics.pdf

Piggott, H. (1997) Windpower Workshop Centre for Alternative Technology Publications, 36-37.

| ISSN: 3065-0712